Hindawi
Advances in Materials Science and Engineering
Volume 2018, Article ID 3240959, 9 pages
https://doi.org/10.1155/2018/3240959

Research Article

Interactive Relationship between Silver Ions and Silver Nanoparticles with PVA Prepared by the Submerged Arc Discharge Method

Kuo-Hsiung Tseng,[1] **Chih-Ju Chou**,[1] **To-Cheng Liu**,[1] **Der-Chi Tien**,[1] **Tong-chi Wu**,[1] **and Leszek Stobinski**[2]

[1]*Department of Electrical Engineering, National Taipei University of Technology, Taipei 10608, Taiwan*
[2]*Materials Chemistry, Warsaw University of Technology, Warynskiego 1, 00-645 Warsaw, Poland*

Correspondence should be addressed to Kuo-Hsiung Tseng; khtseng@ee.ntut.edu.tw

Received 5 June 2017; Revised 12 October 2017; Accepted 9 November 2017; Published 11 January 2018

Academic Editor: Claudio Pettinari

This study uses the submerged arc discharge method (SADM) and the concentrated energy of arc to melt silver metal in deionized water (DW) so as to prepare metal fluid with nanoparticles and submicron particles. The process is free from any chemical agent; it is rapid and simple, and rapid and mass production is available (0.5 L/min). Aside from the silver nanoparticle (Ag^0), silver ions (Ag^+) exist in the colloidal Ag prepared by the system. In the preparation of colloidal Ag, polyvinyl alcohol (PVA) is used as an additive so that the Ag^0/Ag^+ concentration, arcing rate, peak, and scanning electron microscopic (SEM) images in the cases with and without PVA can be analyzed. The findings show that the Ag^0/Ag^+ concentration increases with the addition level of PVA, while the nano-Ag and Ag^+ electrode arcing rate rises. The UV-Vis absorption peak increases Ag^0 absorbance and shifts as the dispersity increases with PVA addition. Lastly, with PVA addition, the proposed method can prepare smaller and more amounts of Ag^0 nanoparticles, distributed uniformly. PVA possesses many distinct features such as cladding, dispersion, and stability.

1. Introduction

The production of nanosized metallic silver particles with different morphologies and sizes using different methods has been reported in previous studies, such as the electric spark discharge system (ESDS) [1–3]. PVA (Mw 89,000–98,000, 99+% hydrolyzed, 341584, 9002-89-5, MDL: MFCD00081922) was the eligible polymer since it stands out for its viscoelastic behavior, hydrophilicity, chemical stability [4] and biocompatibility [5]. PVA contains a large amount of –OH functional groups, which can form chelate composed of metal ions [6]. It is a white powdered resin polymer, with features of viscoelasticity, hydrophilicity, chemical stability, and biocompatibility [7–9]. PVA is used in many medical devices approved by the FDA (Food and Drug Administration, USA) such as contact lenses, membranes, drug delivery systems, and orthopedic devices [10], It is extensively used in biomedical and pharmaceutical applications [11, 12], waste water treatment, and artificial articular cartilages [13]. Initially, we used a biocompatible polymer, PVA, as a reducing agent to convert silver salt ($AgNO_3$) to Ag-NP. Then, we obtained PVA/Ag-NP composite nanofibers via electrospinning [14]. A series of monodispersed Ag-NPs with 25, 35, 45, 60, and 70 nm sizes was reported by using PVP as the surfactant [15]. Also, Ag-NPs can be incorporated within biodegradable poly(lactic acid) [16] or deposited onto modified titanium surfaces [17] as an antibacterial scaffold for tissue engineering and medical applications. Poly(vinyl alcohol) (PVA) is a biodegradable polyester that has been investigated extensively as a biomedical material. Many researchers have utilized electrospinning to fabricate nanofibrous PVA scaffolds for use in wound healing [18–20]. PVA and its nanocomposites have found a wide range of industrial applications such as fiber and textile sizing, coating, adhesives, emulsifiers, and film packaging in food and optical holographic industries [21]. Nevertheless, there were only two articles about PVA/TiO_2 nanocomposite prepared by the ultrasonic irradiation

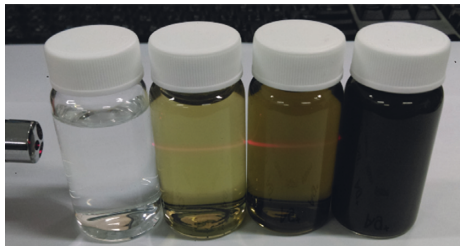

Figure 1: The color of the nanosilver particle suspension changed from yellow to dark brown.

method. To the best of our knowledge [22, 23], high molecular materials, such as PVA [24], by stabilizing with polymer matrix, the silver nanoparticles, are surface modified. Hence, they can also act as capping agents. The homogeneous distribution of silver nanoparticles into the polymer matrix will also increase the surface area and make them fit for catalytic applications. There are several methods to fabricate silver nanoparticle polymer composites [25–27]. Due to PVA's special characteristics, the nano-Ag will distribute uniformly on antibacterial dressings such that the index of the antibacterial dressing becomes more smooth and consistent. The products can be made as a film or gel, or weaved into a fiber.

In recent researches of nanoparticles, it is shown that the color of the Ag nanoparticle, produced by different methods such as presented in literature [28], is getting darker with the increase in concentration, usually from light yellow (since the peak absorption of Ag nanoparticle is 395 nm) to dark brown. In this study, the color of the 10 ppm, 35 ppm, and 60 ppm nanoparticles is light yellow, yellow, and dark brown, respectively, as shown in Figure 1.

2. Research Method and Process

The microelectric discharge machine system comprises the overall mechanism, hardware circuit, power supply, chuck, and so on. The motion control adapter card of the computer is used as the global core. The process performance of parameter setting is observed by changing the arcing rate, thus obtaining the parameter setting for the optimum process efficiency and quality of the nano-Ag colloid. Figure 2 shows the micro-EDM system [29, 30].

2.1. Preparation of Nanosilver by Electrical Spark. This study used SADM to split silver material into nanosized particles by arc discharge. The process was free from chemical agents. Pure solutions, such as pure water, were used as the medium [1].

The silver (99.99% pure) wires with a diameter of 1 mm are used as anode and cathode and are submerged in DW or ethanol. The 200 ml DW is loaded, the positive and negative electrodes are manually fixed and aligned, and then the discharge parameters are set before discharge. The discharge is finished after a period of time, and the product is taken out. The system framework is shown in Figure 3 [3].

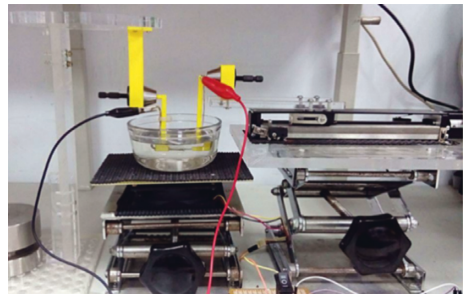

Figure 2: Micro-EDM system.

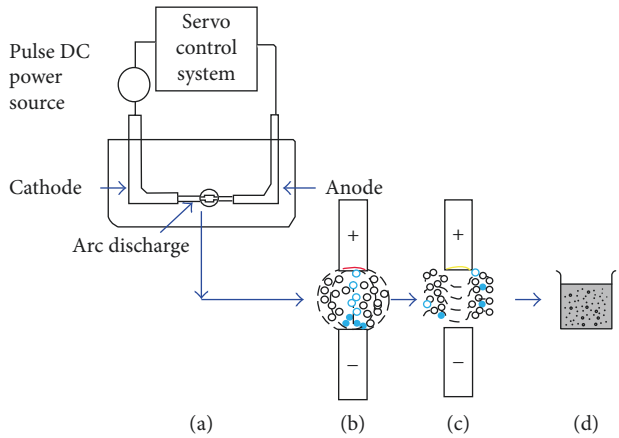

Figure 3: The submerged arc discharge method (SADM) system. (a) SADM system configuration. (b) Ionization and plasma formation. (c) Metal bursts out. (d) Metal particle suspended or precipitated in the dielectric liquid.

Table 1: EDX application for the analysis of the proportion of elements in silver.

Element	Weight (%)	Atomic (%)
C	44.63	57.26
Si	50.64	27.18
O	13.12	12.63
Ag	11.21	1.60
Na	1.08	0.73

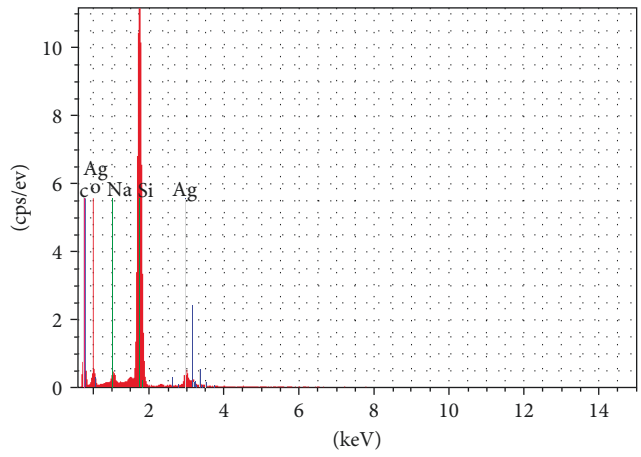

Figure 4: Silver nanoparticle EDX diagram.

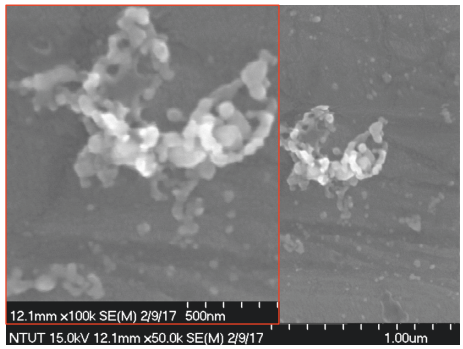

(a)

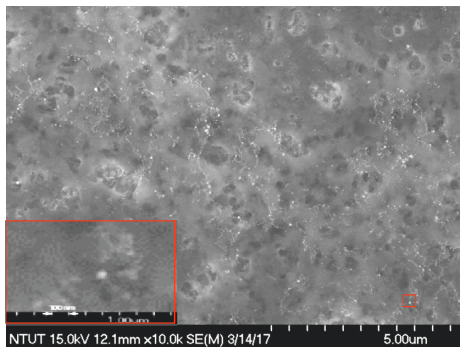

(b)

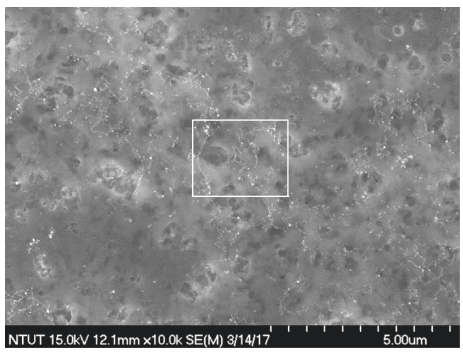

(c)

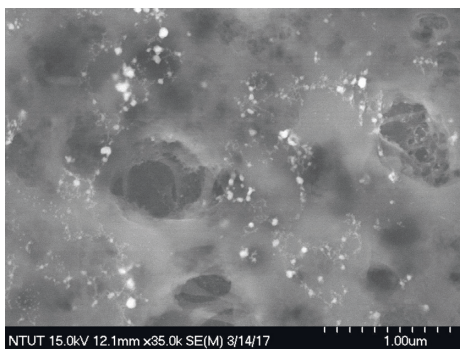

(d)

Figure 5: (a) SEM diagram of aggregated silver nanoparticles. (b) SEM diagram of silver + 0.5% PVA particles. (c) 3D structure of nanocolloid distribution. (d) Zoomed in picture of the 3D structure of the nanocolloid.

Table 2: The measured electrical conductivity versus UV-Vis Ag^+ absorbance at 190–300 nm band.

+PVA (ml)	Electrical conductivity (μs/cm) A (0 min)	B (6 min)	B – A	UV-Vis silver ion peak UV (190–300 nm) band Ag^+ absorbance
2	1.5	2.4	0.9	0.23
4	12.6	21.6	9.0	2.25
6	19.5	33.66	14.2	2.57
8	34.5	52.7	18.2	2.88
10	34.5	59.5	24.9	3.15

Table 3: 2.3 μs/cm (DW) versus 20 μs/cm (with PVA) electrical conductivity basic parameters.

Time/item	0 min (μs/cm)	6 min (μs/cm)	12 min (μs/cm)
Electrical conductivity (water base)	1.5	4.5	—
Electrical conductivity (water + PVA)	17.3	44	60
UV absorbance	0 min	6 min	12 min
UV-Vis 190–300 nm (Ag^+ in PVA base)	1.87	1.2	2.032
UV-Vis 300–600 nm (Ag^0 in PVA base)	0.03	0.814	—
UV-Vis 190–300 nm (Ag^+ peak in water)	0	<190	—
UV-Vis 190–300 nm (Ag^+-PVA^- peak in water)	<190	194	—
UV-Vis 300–600 nm (Ag^0 peak in water)	0	—	394
UV-Vis 300–600 nm (Ag^0-PVA peak in water)	0	—	410
UV-Vis 190–300 nm (Ag^+ in water base)	0	0.227	—
UV-Vis 190–300 nm (Ag^+ in PVA base)	0	2.85	—
UV-Vis 300–600 (Ag^0 in water base)	0	0.247	—
UV-Vis 300–600 (Ag^0 in PVA base)	0	0.899	2.88

2.2. Silver Nanofluid Product Analysis. This study uses DW as a liquid medium to prepare Ag particles. The prepared sample is analyzed by spectrophotometry for the spectral characteristic of the product. The absorbance of nano-Ag colloid is analyzed by spectrophotometry based on the concentration index of nanoparticles. The conductivity of dielectric fluid is measured by a conductivity meter, the purity of dielectric fluid is guaranteed, and the conductivity of general DW is lower than 5.00 μs/cm.

Nanosilver fluid is fabricated. For energy dispersive X-ray spectroscopy (EDX) analysis, a silicon wafer was used as a carrier. Carbon, oxygen, and sodium were typically accompanied with the PVA, and therefore, Ag, C, O, and Na were present. Table 1 and Figure 4 display the EDX analysis results, and SEM analysis is shown in Figures 5(a)–5(d).

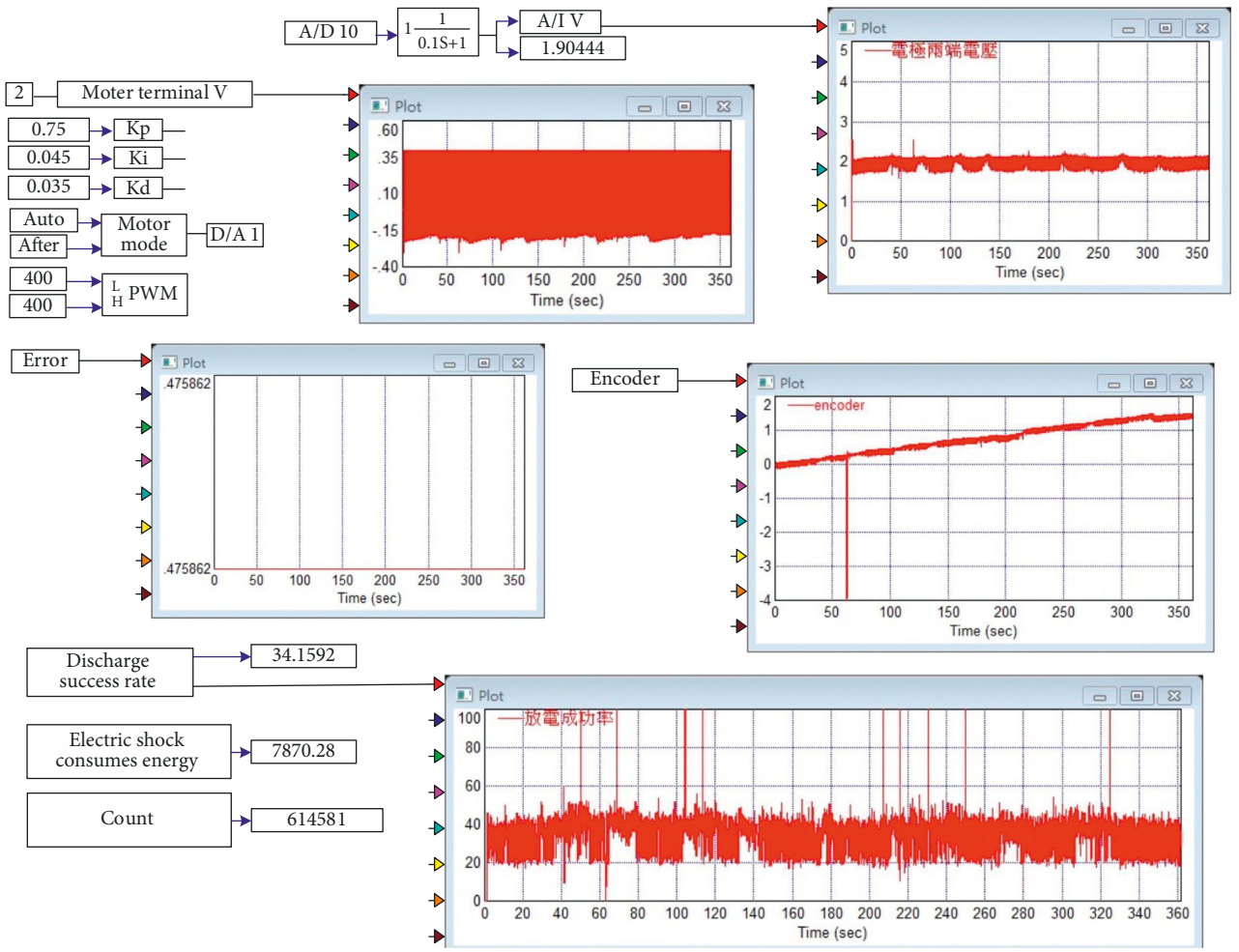

Figure 6: Diagram of Vissim prog. (arcing in DW for 6 min).

3. Experimental Results and Discussion

3.1. Experimental Procedure. The 2.3 μs/cm Ag^+ solution (without PVA) and 20 μs/cm Ag^+ solution (with 10 ml PVA) preparation processes are designed, and the nano-Ag is then prepared at intervals of 6 min. The correlation between Ag^+ and nano-Ag of the nano-Ag colloid and the concentration in the preparation process are defined by electrical conductivity and spectrophotometry (UV-Vis).

3.1.1. Silver Ions. 200 ml DW is mixed with 2 ml, 4 ml, 6 ml, 8 ml, and 10 ml of the PVA, respectively. Ag is driven in 5 min, and the electrical conductivity is measured after the PVA is added to DW. When the PVA addition is 8 ml and 10 ml, the electrical conductivity does not distinctly increase, approaching the saturation concentration, as shown in Table 2.

3.1.2. Silver Ion Solution (with/without PVA). The 2.3 μs/cm Ag^+ solution (DW) and 20 μs/cm Ag^+ solution (with 10 ml PVA) preparation processes are designed. Then, the nano-Ag is prepared at intervals of 6 min. The correlation between Ag^+ and nano-Ag of the nano-Ag colloid and the concentration in the preparation process are defined by electrical conductivity and spectrophotometry (UV-Vis), as shown in Table 3.

3.2. Test Result Analysis

3.2.1. Vissim and UV-Vis. The laboratory report chart of PVA additive in Ag nanoparticle preparation (Vissim and UV-Vis) is shown in Figures 6–11.

3.2.2. Zeta Potential and Size Distribution. The laboratory report chart of PVA additive in Ag nanoparticle preparation (zeta potential and size distribution) is shown in Figures 12–15.

3.3. Results and Discussion. The experimental discussion about the interactive relationship between Ag^+/nano-Ag and PVA is described below.

(1) With PVA, when 8 ml (52.7 μs/cm) or 10 ml (59.5 μs/cm) of DW (200 ml) is added, the electric conductivity has no significant change, meaning that it has reached saturation.

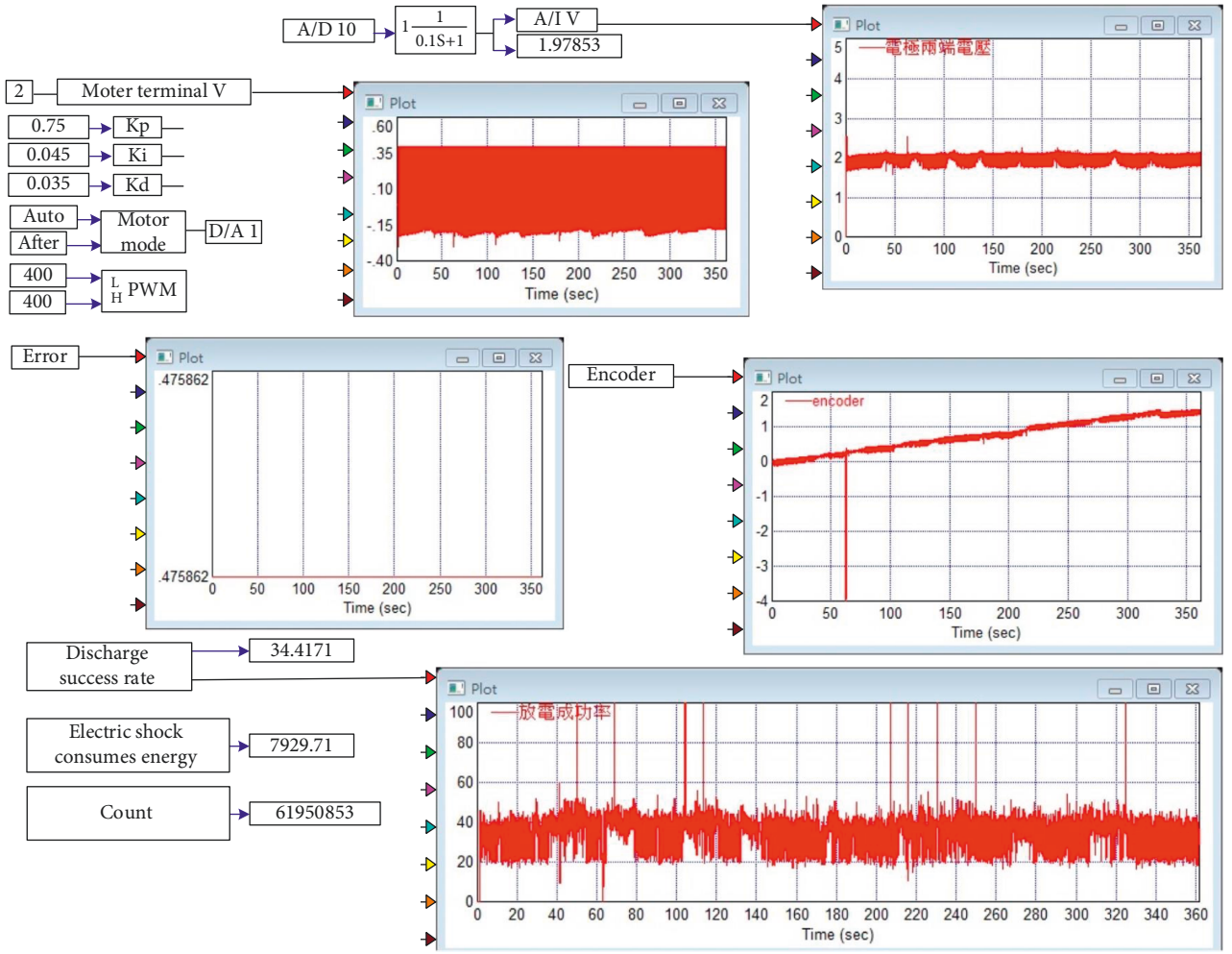

Figure 7: Diagram of Vissim prog. (arcing in DW + PVA for 12 min).

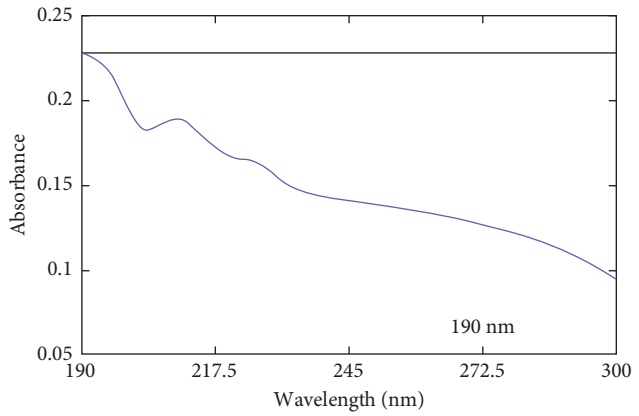

Figure 8: UV-Vis (arcing in DW for 6 min, peak at 190 nm).

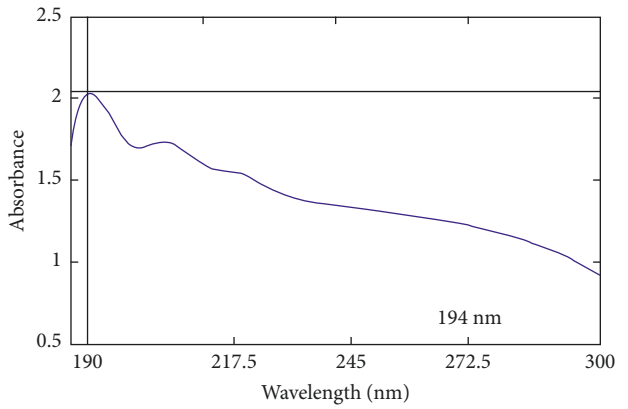

Figure 9: UV-Vis (arcing in DW + PVA for 12 min, peak at 194 nm).

(2) During the discharge process, since the PVA covers the Ag particle and increases the surface charge of the Ag particle, it is seen that, from Figures 6 and 7, the discharging efficiency rises with the increase in the PVA concentration. The diameter of the Ag particle is 30 nm, and it remains 30 nm after the PVA covers the Ag particle; the overall complex may be larger than 30 nm after cladding. This complex is relatively big, and the distance between particles is relatively long. The overall complex is connected after cladding, the complex distance increases, two complexes cannot be

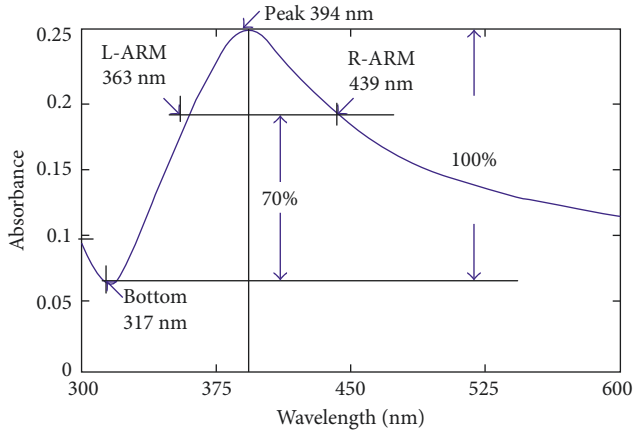

Figure 10: UV-Vis (arcing in DW for 6 min, band width = 76 nm, at absorbance 70% height).

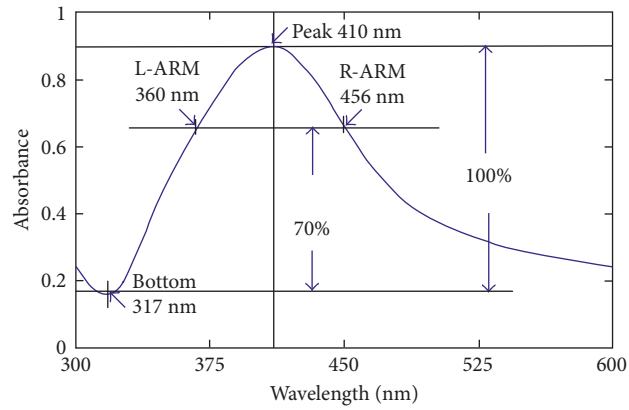

Figure 11: UV-Vis (arcing in DW + PVA for 12 min, band width = 96 nm, at absorbance 70% height).

Results

	Mean (mV)	Area (%)	Width (mV)
Zeta potential (mV) : −26.4	Peak 1: −27.3	90.2	13.0
Zeta deviation (mV): 21.7	Peak 2: 5.70	8.1	4.96
Conductiviy (mS/cm): 0.0186	Peak 3: −82.4	1.0	6.48

Result quality: see result quality report

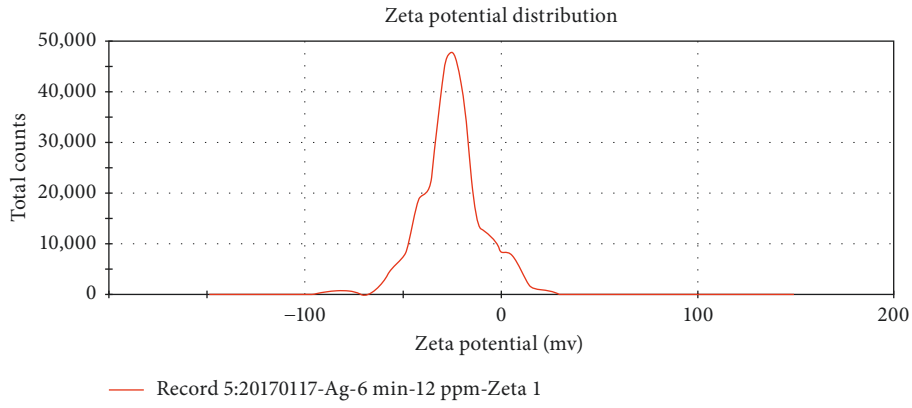

Figure 12: Zeta of aqueous colloid silver (arcing in DW for 6 min).

connected, the covered complex appearance is negatively charged, and each covered complex is negatively charged. The repulsive effect is generated during mutual collision, whereby the negative electric field on the covered complex appearance is higher than the original surface electric field, from 30 mv to 40–45 mv; and the negative electric field on the covered complex appearance is strong so that the covered nano-Ag particles are farther from each other in liquid or colloid. The following situation is tenable. In the same electric field, the farther the Ag particle is, the more unlikely the Ag particle is to cause a short-circuit bridge. As long as the short-circuit bridge does not occur in the discharge process, the controller makes a continuous electrode discharge, and thus, a lot of nano-Ag^0 and Ag^+ are generated so that the electrode consumption per unit time increases.

(3) According to Figure 8, the UV-Vis absorbance peak of DW discharge is driven in $Ag^+ < 190$ nm and the peak of absorption is a waveform < 190 nm (near 190 nm). According to Figure 9, the UV-Vis absorption peak of DW + PVA discharge is driven in $Ag^+ = 194$ nm. According to Figures 8 and 9, the UV absorbance peak of DW + PVA shifts right. Carefully inspecting Figures 8 and 9, it is obvious that Ag^+ may shift right under the addition of PVA introduced. This is the first breakthrough of the current study.

(4) According to Figure 10, in the case of DW-Ag^0 (6 min), Ag^0 surrounds the AgOH and Ag_2O, and the corresponding wavelength of UV-Vis absorbance peak is 394 nm. As shown in Figure 11, when the Ag^0 surrounds the Ag^+-PVA^- compound, the corresponding wavelength of absorption peak in the UV-Vis (300–600) spectrum is 410 nm, and the UV-Vis

	Results		
	Mean (mV)	Area (%)	Width (mV)
Zeta potential (mV): −38.6	Peak 1: −38.2	98.5	11.0
Zeta deviation (mV): 11.6	Peak 2: −74.3	1.5	4.10
Conductivity (mS/cm): 0.0514	Peak 3: 0.00	0.0	0.00
Result quality: good			

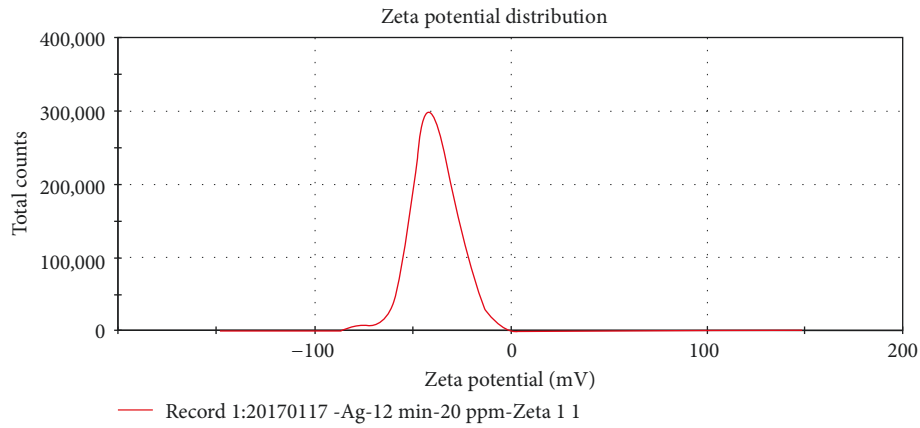

Figure 13: Zeta of aqueous colloid silver (arcing in DW + PVA for 12 min).

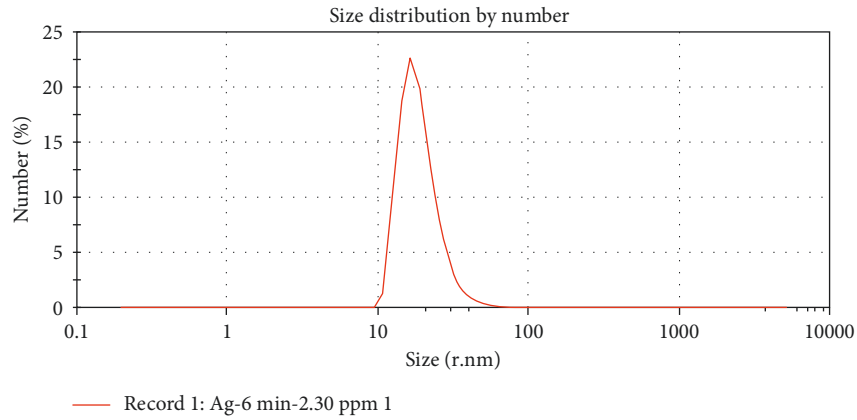

Figure 14: Particle size distribution of aqueous colloid silver (arcing in DW for 6 min).

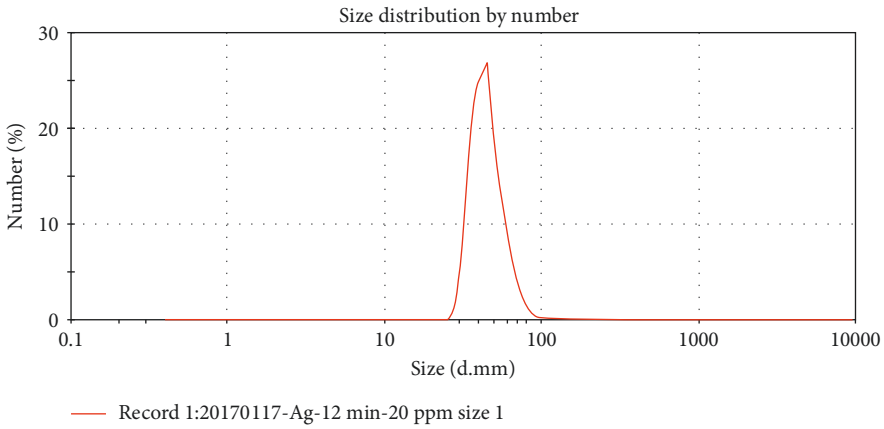

Figure 15: Particle size distribution of aqueous colloid silver (arcing in DW + PVA for 12 min).

(190–300) absorption peak increases to at least 1.2. This suggests that the Ag^+ concentration rises to 12 ppm, and 1 ppm in general approximates to 1 μm/cm. The total electrical conductivity is 24 μm/cm, meaning at least 12 μm/cm of the concentration results from Ag^+ and the rest of 12 μm/cm results from the PVA derivant. Figures 10 and 11 indicate that the DW-Ag^0 (6 min) wavelength is 76 nm at absorbance 70%, and the PVA (6 min) wavelength is 94 nm at absorbance 70%. Another new finding is that the particle size is measured by the Zetasizer. It is deduced that the Ag^0 complex is combined with PVA, which leads to increase in the equivalent diameter, thus causing the peak of Ag^0 shifting from 394 nm to 410 nm. Moreover, at the neck of the UV-Vis absorbance wavelength 70% in Figures 10 and 11, the wavelength of DW-Ag^0 (6 min) is 76 nm. The width of the neck of DW + 0.5%/w/w-Ag^0 (6 min) UV-Vis wavelength at 70% is 96 nm. This is because the (Ag^+-PVA^-) complex makes the overall Ag^0 UV-Vis spectrum neck width wavelength increase from 76 nm to 96 nm.

(5) According to Figures 14 and 15, the particle size and distribution are 50–100 nm in the DW solution without PVA. When (0.05%/w/w) PVA is added, the particle diameter is 25–75 nm.

4. Conclusion

The experimental results about the interactive relationship between Ag^+/Nano-Ag and PVA are described below.

(1) According to the increment ratio of electrical conductivity and absorption peak in the experiment, the PVA is correlated to the Ag^0/Ag^+ concentration.

(2) As the electrode discharges continuously, a lot of Ag^0 and Ag^+ are generated, and the electrode consumption per unit time increases, so that the Ag^0 and Ag^+ arcing rate rises.

(3) When Ag^+ is combined with PVA (0.05%/w/w), it forms a ($Ag^+ \cdot PVA^-$) compound. The molecular weight of this compound is much heavier than $(Ag^+)_2O^-$ and Ag^+OH^-, and the absorption peak of Ag^+ shifts right to 194 nm.

(4) The PVA not only helps the formation of Ag^+ but also increases the formation of Ag^0. After the PVA is added, the concentration of Ag^+ increases 5 times (1.2/0.227 = 5.28) and Ag^0 increases 3 times (0.899/0.247 = 3.63). Here, Ag^0 is covered by PVA, increasing its dispersity and forming the Ag^+-PVA^- compound. The neck width of Ag^0 on the UV-Vis absorbance wavelength at the height of 70% shifts from 76 nm to 96 nm, with its Ag^0 peak shifting from 394 nm to 410 nm.

(5) According to SEM image in Figures 5(a) and 5(b), the particle agglomeration is severe before the Ag^0 is mixed with PVA. The particles have irregular shape, and the particle size and distribution are nonuniform. When 0.5% PVA is added in, the particle size becomes smaller and is distributed over the PVA surface uniformly. Meanwhile, the surface zeta potential of Ag^0 increases, and the catalytic activity rises, so that the Ag-PVA complex is easier to disperse.

Conflicts of Interest

The authors declare that there are no conflicts of interest regarding the publication of this paper.

References

[1] K.-H. Tseng, H.-L. Lee, D.-C. Tien, Y.-L. Tang, and Y.-S. Kao, "A study of antibioactivity of nanosilver colloid and silver ion solution," *Advances in Materials Science and Engineering*, vol. 2014, Article ID 371483, 6 pages, 2014.

[2] K.-H. Tseng, H.-L. Lee, C.-Y. Liao, K.-C. Chen, and H.-S. Lin, "Rapid and efficient synthesis of silver nanofluid using electrical discharge machining," *Journal of Nanomaterials*, vol. 2013, Article ID 174939, 6 pages, 2013.

[3] K.-H. Tseng, C.-J. Chou, T.-C. Liu, Y.-H. Haung, and M.-Y. Chung, "Preparation of Ag-Cu composite nanoparticles by the submerged arc discharge method in aqueous media," *Japan Institute of Metals and Materials Transactions*, vol. 57, no. 3, pp. 294–301, 2016.

[4] R. Tamaki and Y. Chujo, "Synthesis of poly(vinyl alcohol)/silica gel polymer hybrids by in-situ hydrolysis method," *Applied Organometallic Chemistry*, vol. 12, no. 10-11, pp. 755–762, 1998.

[5] S. R. Sudhamani, M. S. Prasad, and K. U. Sankar, "DSC and FTIR studies on gellan and polyvinyl alcohol (PVA) blend films," *Food Hydrocolloids*, vol. 17, no. 3, pp. 245–250, 2003.

[6] L. A. García-Cerda, M. U. Escareno-Castro, and M. Salazar-Zertuche, "Preparation and characterization of polyvinyl alcohol-cobalt ferrite nanocomposites," *Journal of Non-Crystalline Solids*, vol. 353, no. 8–10, pp. 808–810, 2007.

[7] M. I. Baker, S. P. Walsh, Z. Schwartz, and B. D. Boyan, "A review of polyvinyl alcohol and its uses in cartilage and orthopedic applications," *Journal of Biomedial Materials Research Part B: Applied Biomaterials*, vol. 100, no. 5, pp. 1451–1457, 2012.

[8] K. Ng, P. A. Torzilli, R. F. Warren, and S. A. Maher, "Characterization of a macroporous polyvinyl alcohol scaffold for the repair of focal articular cartilage defects," *Journal of Tissue Engineering and Regenerative Medicine*, vol. 8, no. 2, pp. 164–168, 2014.

[9] S. Jiang, S. Liu, and W. Feng, "PVA hydrogel properties for biomedical application," *Journal of the Mechanical Behaviour of Biomedical Materials*, vol. 4, no. 7, pp. 1228–1233, 2011.

[10] B. Bolto, T. Tran, M. Hoang, and Z. Xie, "Crosslinked poly (vinyl alcohol) membranes," *Progress in Polymer Science*, vol. 34, no. 9, pp. 969–981, 2009.

[11] C. M. Hassan and N. A. Peppas, "Structure and applications of poly(vinyl alcohol) hydrogels produced by conventional crosslinking or by freezing/thawing methods," *Advances in Polymer Science*, vol. 153, pp. 37–65, 2000.

[12] S. Mollazadeh, J. Javadpour, and A. Khavandi, "In situ synthesis and characterization of nano-size hydroxyapatite in poly(vinyl alcohol) matrix," *Ceramics International*, vol. 33, no. 8, pp. 1579–1583, 2007.

[13] L. I. Xinming and C. U. I. Yingde, "Study on synthesis and chloramphenicol release of poly(2-hydoxyethylmethacrylate-

co-acrylamide) hydrogels," *Chinese Journal of Chemical Engineering*, vol. 16, no. 4, pp. 640–645, 2008.

[14] A. Celebioglu, Z. Aytac, O. C. O. Umu, A. Dana, T. Tekinay, and T. Uyar, "One-step synthesis of size-tunable Ag nanoparticles incorporated in electrospun PVA/cyclodextrin nanofibers," *Carbohydrate Polymers*, vol. 99, pp. 808–816, 2014.

[15] G. K. Vertelov, Y. A. Krutyakov, O. V. Efremenkova, A. Y. Olenin, and G. V. Lisichkin, "A versatile synthesis of highly bactericidal Myramistin® stabilized silver nanoparticles," *Nanotechnology*, vol. 19, no. 35, p. 355707, 2008.

[16] Y. Zhang, H. Peng, W. Huang, Y. Zhou, and D. Yan, "Facile preparation and characterization of highly antimicrobial colloid Ag or Au nanoparticles," *Journal of Colloid and Interface Science*, vol. 325, no. 2, pp. 371–376, 2008.

[17] L. Li, J. Sun, X. Li et al., "Controllable synthesis of monodispersed silver nanoparticles as standards for quantitative assessment of their cytotoxicity," *Biomaterials*, vol. 33, no. 6, pp. 1714–1721, 2012.

[18] N. Charernsriwilaiwat, P. Opanasopit, T. Rojanarata, and T. Ngawhirunpat, "Lysozyme-loaded, electrospun chitosan-based nanofiber mats for wound healing," *International Journal of Pharmaceutics*, vol. 427, no. 2, pp. 379–384, 2012.

[19] C. Cencetti, D. Bellini, A. Pavesio et al., "Preparation and characterization of antimicrobial wound dressings based on silver, gellan, PVA and borax," *Carbohydrate Polymers*, vol. 90, no. 3, pp. 1362–1370, 2012.

[20] T. Nitanan, P. Akkaramongkolporn, T. Rojanarata, T. Ngawhirunpat, and P. Opanasopit, "Neomycin-loaded poly(styrene sulfonic acid-co-maleic acid) (PSSA-MA)/polyvinyl alcohol (PVA) ion exchange nanofibers for wound dressing materials," *International Journal of Pharmaceutics*, vol. 448, no. 1, pp. 71–78, 2013.

[21] V. Goodship and E. Ogur, *Polyvinyl Alcohol: Materials, Processing and Applications*, Smithers Rapra Technology, vol. 16, Shrewsbury, UK, 2005.

[22] Y. Lou, M. Liu, X. Miao, L. Zhang, and X. Wang, "Improvement of the mechanical properties of nano-TiO_2/poly (vinyl alcohol) composites by enhanced interaction between nanofiller and matrix," *Polymer Composites*, vol. 31, no. 7, pp. 1184–1193, 2010.

[23] M. Sairam, M. B. Patil, R. S. Veerapur, S. A. Patil, and T. Aminabhavi, "Novel dense poly(vinyl alcohol)–TiO_2 mixed matrix membranes for pervaporation separation of water-isopropanol mixtures at 30°C," *Journal of Membrane Science*, vol. 281, no. 1-2, pp. 95–102, 2006.

[24] G. A. Gaddy, A. S. Korchev, J. L. Mclain, B. L. Slaten, E. S. Steige rWalt, and G. Mills, "Light-induced formation of silver particles and clusters in cross linked PVA/PAA films," *Journal of Physical Chemistry B*, vol. 108, no. 39, pp. 14850–14857, 2004.

[25] P. K. Khanna, N. Singh, S. Charan, V. V. V. S. Subbarao, R. Gokhale, and U. P. Mulik, "Synthesis and characterization of Ag/PVA nanocomposite by chemical reduction method," *Materials Chemistry and Physics*, vol. 93, no. 1, pp. 117–122, 2005.

[26] S. Park, D. Seo, and J. Lee, "Preparation of Pb-free silver paste containing nanoparticles," *Colloids and Surfaces A: Physicochemical and Engineering Aspects*, vol. 313-314, pp. 197–201, 2008.

[27] K. Park, D. Seo, and J. Lee, "Conductivity of silver paste prepared from nanoparticles," *Colloids and Surfaces A: Physicochemical and Engineering Aspects*, vol. 313-314, pp. 351–354, 2008.

[28] Z. Zengsheng, L. Xianxue, G. Zhenyu, and L. Yujie, "Silver silver," *Scientific Development*, vol. 408, pp. 32–39, 2006.

[29] K.-H. Tseng, C.-Y. Liao, J.-C. Huang, D.-C. Tien, and T.-T. Tsung, "Characterization of gold nanoparticles in organic or inorganic medium (ethanol/water) fabricated by spark discharge method," *Materials Letters*, vol. 62, no. 19, pp. 3341–3344, 2008.

[30] K.-H. Tseng, Y.-S. Kao, and C.-Y. Chang, "Development and implementation of a micro-electric discharge machine: real-time monitoring system of fabrication of nanosilver colloid," *Journal of Cluster Science*, vol. 27, no. 2, pp. 763–773, 2016.